Journal of Hydrology 524 (2015) 522–537

Contents lists available at ScienceDirect

Journal of Hydrology

journal homepage: www.elsevier.com/locate/jhydrol

Analysis of flood modeling through innovative geomatic methods

Santiago Zazo *, José-Luis Molina, Pablo Rodríguez-Gonzálvez

Salamanca University, High Polytechnic School of Engineering, Ávila. Area of Hydraulic Engineering, Av. de los Hornos Caleros, 50, 05003 Ávila, Spain

ARTICLE INFO

Article history:
Received 26 December 2014
Received in revised form 21 February 2015
Accepted 5 March 2015
Available online 14 March 2015
This manuscript was handled by Geoff Syme, Editor-in-Chief

Keywords:
Flood modeling Reduced Cost Aerial Precision Photogrammetry (RC-APP)
Hydraulics
Geomatic
Aircraft Ultra-Light Motor (ULM)

SUMMARY

A suitable assessment and management of the exposure level to natural flood risks necessarily requires an exhaustive knowledge of the terrain. This study, primarily aimed to evaluate flood risk, firstly assesses the suitability of an innovative technique, called Reduced Cost Aerial Precision Photogrammetry (RC-APP), based on a motorized technology ultra-light aircraft ULM (Ultra-Light Motor), together with the hybridization of reduced costs sensors, for the acquisition of geospatial information. Consequently, this research generates the RC-APP technique which is found to be a more accurate–precise, economical and less time consuming geomatic product. This technique is applied in river engineering for the geometric modeling and risk assessment to floods. Through the application of RC-APP, a high spatial resolution image (orthophoto of 2.5 cm), and a Digital Elevation Model (DEM) of 0.10 m mesh size and high density points (about 100 points/m^2), with altimetric accuracy of −0.02 ± 0.03 m have been obtained. These products have provided a detailed knowledge of the terrain, afterward used for the hydraulic simulation which has allowed a better definition of the inundated area, with important implications for flood risk assessment and management. In this sense, it should be noted that the achieved spatial resolution of DEM is 0.10 m which is especially interesting and useful in hydraulic simulations through 2D software. According to the results, the developed methodology and technology allows for a more accurate riverbed representation, compared with other traditional techniques such as Light Detection and Ranging (LiDAR), with a Root-Mean-Square Error (RMSE ± 0.50 m). This comparison has revealed that RC-APP has one lower magnitude order of error than the LiDAR method. Consequently, this technique arises as an efficient and appropriate tool, especially in areas with high exposure to risk of flooding. In hydraulic terms, the degree of detail achieved in the 3D model, has allowed reaching a significant increase in the knowledge of hydraulic variables in natural waterways.

1. Introduction

The availability of surface water in terms of quality, reliability and safety to people, properties and dependent productive activities, is crucial to any society. There is some consensus in the scientific community that achieving this is only possible through a sustainable resource use within an integrated exploitation framework. This is the international paradigm of performance and analysis of water studies, known as "Integrated Water Resources Management" (IWRM) (Molina et al., 2013).

The reality of climate change, expressed in terms of occurrence of extreme hydrological events, produces a stronger pressure on water resources systems (Chávez Jiménez, 2012; Molina et al., 2013) and the physical environment (Ashley et al., 2005). Consequences on the terrain are slowly conducting the society to take effective protective and adaptive interventions (EU Directive, 2007; Zechner et al., 2011). Most of these interactions are being currently studied in research through non-structural actions (Escuder-Bueno et al., 2012). For that, the decision making on water resources management should include economic considerations, involving the search for a maximum efficiency in the analysis and design of solutions (Sayers et al., 2002). Given this situation, it becomes necessary to have a set of efficient and flexible tools, techniques and methodologies, to facilitate the process of decision making and solutions design.

For a correct assessment of exposure level to natural flood risks is crucial obtaining a detailed-accurate reconstruction of the terrain susceptible to be affected, which provides a proper inundation modeling. In Spain, floods are a natural disaster causing considerable damage, estimated to total about 800 million Euros per year (0.08% of GDP). According to the Consortium of secured property, in the period 1971–2012, 42.9% of the cases processed were due to flood damage, which have accounted for 60.3% of total compensation (MAGRAMA, 2014).

* Corresponding author.
E-mail address: szazo@usal.es (S. Zazo).

http://dx.doi.org/10.1016/j.jhydrol.2015.03.011
0022-1694/

Nowadays, data acquisition and generation of accurate and reliable geomatic products, in the field of fluvial hydraulics and hydrodynamics, was carried out with costly instrumentation, equipment and platforms (Bates et al., 2003; Garcia-Pintado et al., 2013; Horritt and Bates, 2001; Tsubaki and Fujita, 2010; Turner et al., 2013), requiring highly specialized work teams, with very rigid technical constraints that prolong the process of decision making.

Having data in a quick and accurate way is usually associated with a higher cost. On the contrary, lower cost is usually accompanied by low accuracy and less reliable representation of the terrain, which is directly transmitted to the analysis/risk assessment (Merwade et al., 2008b), and design solutions, with their subsequent economic implications.

However, the new paradigms of geomatic science, result of the progress achieved in the last three decades, provide the scientific and engineering community of a set of reduced cost and even low cost techniques and methodologies. This, directly impacts on more efficient use of economic resources affecting at public administrations and private corporations.

Some of the computer advances in geomatic materialize in aerial imagery processing software, characterized by friendly, sequential, and to some extent automated workflows. This enables non-geomatic expert's users, process their own dataset, configured as an efficient alternative, to the highly specialized professional photogrammetric software packages.

This case study is aimed to assess the suitability of hybrid low-cost sensors, embarked in alternative aerial platforms (lightweight, low speed and suitable for manned flight) of ULM type (Ultra-Light Motor). This, together with the innovative image processing software, gives some alternatives ways in the sphere of river engineering, applied to the modeling and analysis of flow and flood risk assessment. This innovative technique is called Reduced Cost Aerial Precision Photogrammetry (RC-APP).

2. State of the art

The modeling of flooding is characterized by the relationship between flow and physical environment. The surface flow is a physical phenomenon that presents a great randomness in frequency and magnitude, which makes it deterministically unpredictable. For a better assessment and prediction, stochastic models in form of probability (probabilistic distributions or functions) are used in rainfall-runoff modeling (Martínez and Salas, 2004; Ng and Panu, 2010) and, they are indirectly also subjects of this research. Since precipitation is practically pure random process, and physical environment also is random itself, this stochasticity is twofold. Furthermore, land uses and modifications of the terrain and vegetation cover are associated to seasonality. On the other hand, the terrain is the physical support or container of hydrological–hydraulic processes, where the hydrological cycle is related to the environment and humans (Andreu, 1993). The manifestation of the basin behavior related to the hydrological cycle is produced as runoff surface, or as flooding, when the carrying capacity of rivers or channels is exceeded, when hydrological extreme events occur or when infrastructure is not correctly designed.

Nowadays, there is a relative consensus among researchers and engineers on the knowledge of the physical and hydraulic surface hydrology principles, which has enabled water resources planning and management (Balairón Pérez, 2002; Biswas and Tortajada, 2003). However, it should not be overlooked that extreme events are becoming more recurrent over time and consequently, they are less anomalous events over the time. This brings serious consequences on water resources systems functioning (Bates et al., 2008; Estrela et al., 2012), surface hydrology (Dawson et al., 2005) and groundwater (Molina et al., 2013), which makes the climatic variables even more unpredictable, generating more uncertainty.

The accuracy in the definition of flooding is an essential factor, in cartographic and globally terms (Merwade et al., 2008b; Wechsler, 2007; Bales and Wagner, 2009; Jung and Merwade, 2012). The influence of the riverbed terrain and how it has been obtained should not be overlooked in the results of hydraulic simulations (Cook and Merwade, 2009). For this reason, the research is focused on the flooding from the perspective of the physical environment.

The variety of geomatic techniques for data acquisition in modeling flow sensors are exposed and detailed intensively in the study (Molina et al., 2014), where also the precision of each is indicated. In this sense, in the last 30 years, there has been a constant revolution consequence of hybridization between techniques and sensors, as an example the developments in LiDAR (Light Detection and Ranging) exposed in (Irish and White, 1998).

This degree of development has originated, in the last decades of the twentieth century, the appearance of Digital Photogrammetry (DP), as a discipline of geomatic science. DP is fully integrated into many scientists and technicians, such as civil engineering, building, energy, risk assessment, robotics, an even medicine. The main reason is that the photographic image can provide complete information about the object being studied, including metric level and having an image (Gonzalez-Aguilera and Gomez-Lahoz, 2008).

Technological advances in remote sensing and geomatic techniques, in the field of hydraulics and river engineering, are focused on the use of different type of images, mentioned as follows. High spatial resolution, Very High Resolution images (VHR imagery) of 5–10 cm spatial resolution (Lejot et al., 2007), LiDAR Digital Elevation Models (DEM), with nominal accuracies from ±0.15 m to ±0.25 m (Lane et al., 2003), classic surveying with accuracy of ±0.05 m (Prinos, 2008), the use of observations Synthetic Aperture Radar (SAR) as a source of calibration flood modeling (Horritt and Bates, 2001), and the use of innovative aerial platforms low flying height, Unmanned Aerial Vehicles (UAV) (Vallet et al., 2011), which allow high spatial resolutions, but have a set of limitations, technical and administrative described in (Hardin and Jensen, 2011; Watts et al., 2010). The temporary flight restriction penalizes its applicability in river studies as it is shown in (Ortega-Terol et al., 2014), with a study case length of 132 km.

In order to generate flood risk maps, the construction of continuous Digital Terrain Model (DTM) is essential. In this case, it is common the integration of geometric data from different sources (Prinos, 2008), such as Topographic and Bathymetric LiDAR, classic surveying, with different accuracies (Molina et al., 2014), and the combination of these, through grids (Raster/GRID) and Triangular Irregular Network (TIN) (Merwade et al., 2008b).

On the other hand, Geographic Information Systems (GIS) as a procedural and integrated tool, applied as a physical terrain support for modeling flows are fully seated in the scientific and engineering community, as seen in (Chen et al., 2009; Liu et al., 2014; Merwade et al., 2008a; Wiles and Levine, 2002). Likewise the combination of geomatic techniques and GIS, in the geometric study of riverbeds can be viewed in works such as (Bates and De Roo, 2000; Marcus and Fonstad, 2008). However, the majority of the work and studies have in common that the acquisition of geometric information is from aerial platforms and/or satellite with onboard sensors, in both cases, high cost (Bates and De Roo, 2000; Legleiter and Overstreet, 2012; Marcus and Fonstad, 2010). For example, an individual high spatial resolution satellite image, up to 0.25 m, could cost around € 7000 (Airbus Defense & Space and Infoterra SGSA, 2015), with a minimum area of 14.8 km^2 (4 × 3.7 km). This minimum area can be much higher than the one needed for the study case, and it may be possible to require more than one image, due to the specific characteristics of the sensor data acquisition protocol.

Furthermore, regarding technical resources, precisions, errors and limitations, this study is framed within a context of economic efficiency. The first goal is generating specific geomatic products of high accuracy (−0.02 ± 0.03) m, with a lower magnitude order or error than the usual methods. Consequently, this speeds up the process of data acquisition and decision making in the field of fluvial hydraulics with the minimum environmental impact and to be applied on large riverbeds surfaces and lengths, up to 130 km (Ortega-Terol et al., 2014).

At this point, it has been investigated the applicability of innovative MUSAS® (Multispectral Sensors Airborne System), operated in a platform of light flying, ULM type (tandem trike) and processed with photogrammetric software (an innovative application of this software in natural resources management field), aerial imagery, for the generation of orthophotos and 3D models of riverbeds. The MUSAS® platform can ship multiple sensors, acquiring data within different spectral regions (visible, infrared, thermal, ...), although in this study only the visible spectrum was used.

3. Case study

The study is aimed to apply simulations of stream flow and flood modeling for the analysis, assessment and defense against flooding (Tsakiris, 2014). For that, certain hydrological–geometrical specifications have been considered regarding flows through the central channel cross section.

The case study comprises a surface of 0.50 km^2, and a riverbed stretch length of 3.9 km. The area is nominated as "special interest" in the municipality of El Fresno (Fig. 1), located about 6.5 km upstream the city of Ávila in the province of Avila (Spain).

The study area is located in the Amblés Valley, Upper Basin of the Adaja River, SW of the city of Ávila, north of the Central System, in the northern Spanish plateau, where this stream comprises the main riverbed. This subsystem is integrated within the Duero River Basin (the largest basin in the Iberian Peninsula, in terms of surface).

The point of assessment for hydraulic flow simulations (X = 351829 m, Y = 4497706 m EPSG 25830) determines a watershed of 530 km^2 versus 740 km^2 of the total surface of the Upper Basin of the Adaja river.

In the analyzed stretch, on the right bank, the village center as well as basic municipal utilities (water, sanitation, electricity and telecommunications), sports facilities and recreational areas are located. Likewise, on the left bank, there are several farms and livestock, scattered buildings, and a bridge over the riverbed.

There is a range of altitudes, between 1500 m a.s.l and 1070 m a.s.l. As regards climate of the basin, this is characterized by a cold Mediterranean climate, high continental, with moderately warm summers and severe winters, where the altitude conditions the temperature, with a mean annual of 11 °C. Rainfall patterns are scarce and irregular, consequence of the Foehn effect, with an average annual value of about 400 mm.

4. Methodology

This research has a double fluvial hydraulic and geomatic component articulated in 4 stages, problem definition,

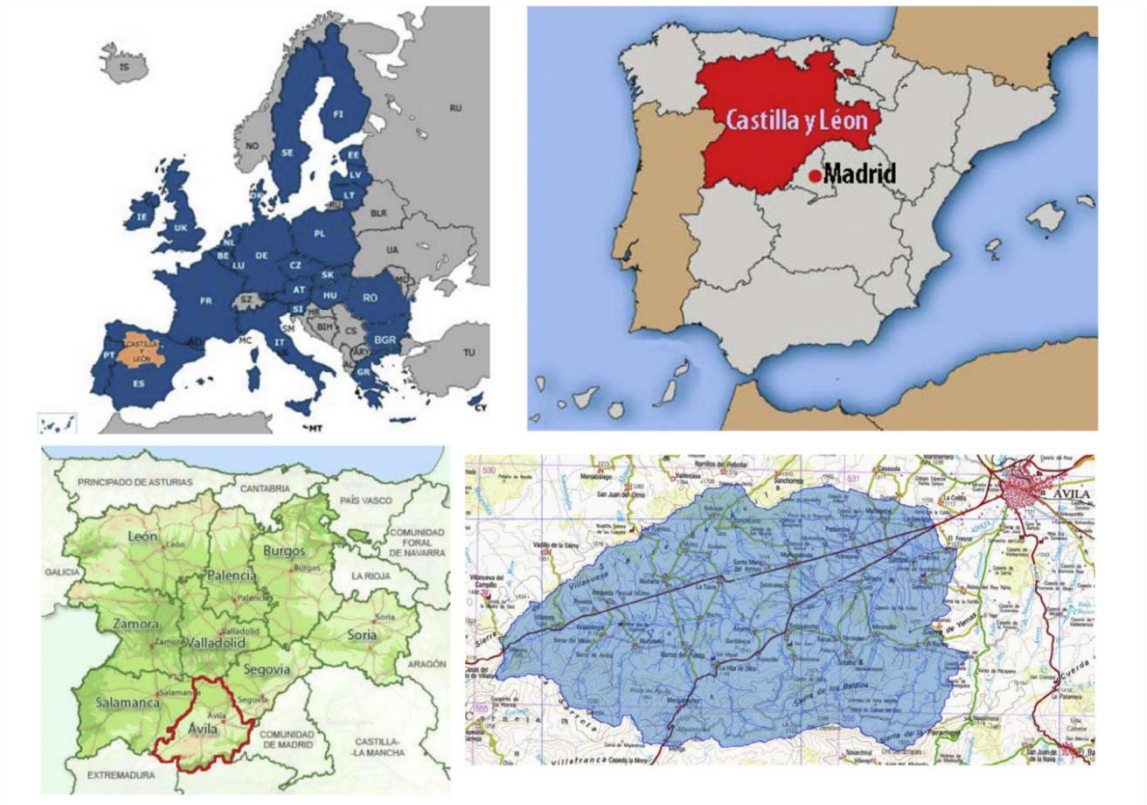

Fig. 1. Situation and basin.

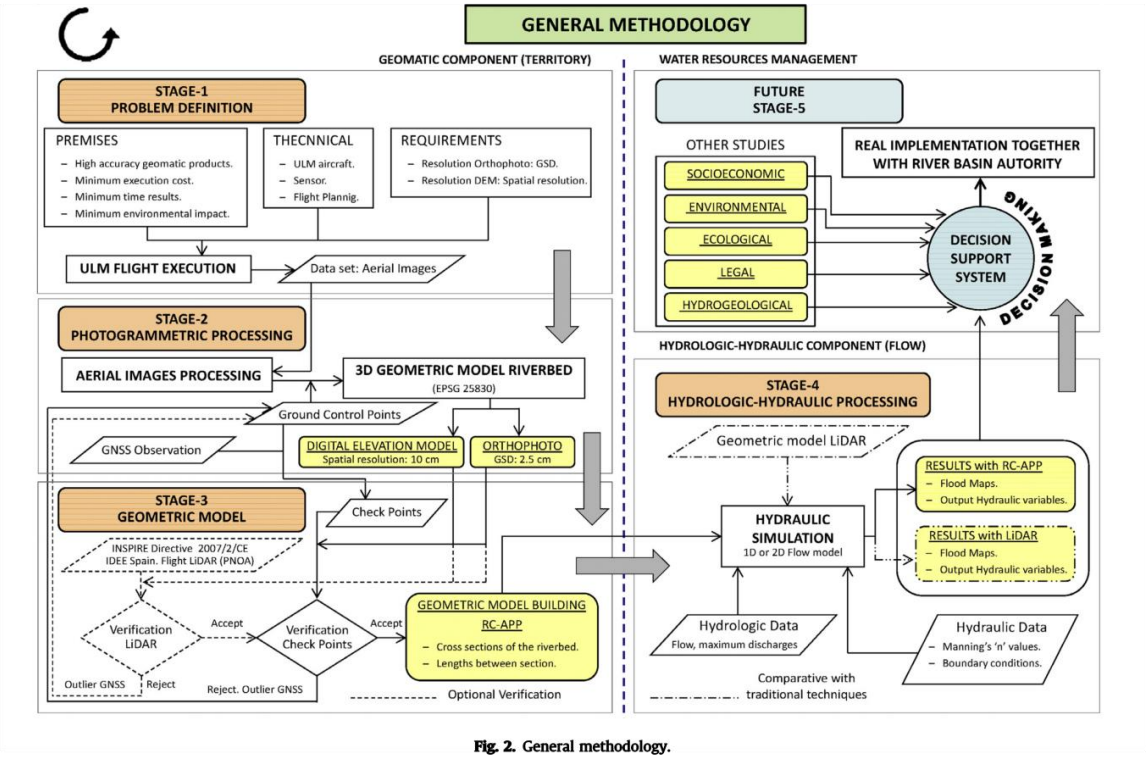

Fig. 2. General methodology.

photogrammetric processing, geometric model and hydrological–hydraulic process, and finally a fifth stage about future research (Fig. 2).

4.1. Stage-1. Problem definition

In this initial stage, the objectives, constraints and technology to apply are formulated and defined. For accurate modeling of floods is essential to have a detailed continuous geometric model the riverbed (Merwade et al., 2008a), given the significant importance of the terrain on the result of fluvial modeling (Merwade et al., 2008b; Wechsler, 2007). This task is reached by the making of an orthophoto and a Digital Elevation Model (DEM). For that it is necessary to define, *a priori*, their resolution, establishing resolutions of 2.5 cm for the orthophoto, and 0.10 m for the DEM. According to previous empirical studies (Zazo and Rodríguez-Gonzálvez, 2014), this is the way to suitably represents the riverbed 3D model and possible structures and existing buildings, and it decisively drive the flow analysis.

The workflow presented in this section is optimized according to: (a) the requirements of accuracy, (b) the processing time to improve the process of decision making and (c) the environmental impact.

The optimal technique for acquiring the geometry of the riverbed is affected by the environmental conditions of the case study. The low and seasonal rainfall, leading to a severe and long (several months a year) dry period with no surface flow in the riverbed, enabling total inspection of the riverbed. This inspection is made with a single technique, and without using bathymetric techniques to represent the riverbed, which certainly allows for better modeling of flooding, as set out in Cook and Merwade (2009) and Merwade et al. (2008b).

For choosing the most suitable technique, it was considered that LiDAR elevation errors may be biased presenting systematic errors (Aguilar and Mills, 2008; Cooper et al., 2013). In studies, such as (Kraus and Pfeifer, 1998; Schmidt et al., 2011), these errors show a negative bias, in contrast to the studies where the bias is positive (Adams and Chandler, 2002; Hodgson et al., 2005). Consequently, since it may produce lack of definition on the inundated area, this bias has important consequences for the floods modeling.

Within the context of maximum efficiency (time-cost) and considering the following: (a) suitability assessment of geomatic methods based on photogrammetric techniques (Molina et al., 2014), (b) assessing accuracy values and spatial resolution, according to previous empirical studies (Zazo and Rodríguez-Gonzálvez, 2014), (c) the singular seasonality of the study area, and (d) the problem regarding bias of LiDAR data (Cooper et al., 2013), RC-APP technique can be considered as one of the most suitable geomatic technique. In order to support the previous statement, technical characteristics of geomatic products, their temporal availability and suitability assessment are outlined in Table 1.

Cost factor is an important decision variable on the technique choice. Acquired data from satellite platforms require large minimum areas (Airbus Defense & Space and Infoterra SGSA, 2015), and also, the acquisition constraint about the minimum area extension, are important disadvantages. Because of this, the associated cost to this data source is extremely high, and it is not appropriate for small study areas. Regarding LiDAR platforms, boarded on aircraft or helicopter, their costs are also important, because of, in both cases, the high mobilization costs. According to (Haugerud et al., 2009), the relationship between the final cost and the surveyed area follows a negative exponential curve. For areas between 130 and 260 km^2 the final cost per hectare is the

Table 1
Main characteristic of techniques for flood modeling.

Technique	Geomatic products		Temporal availability	Suitability
	Orthophoto GSD[f]	DEM Altimetric resolution		
Satellite[a]	Max. 0.25 m	2–0.5 m	About 30 days	Low
LiDAR[b]	Max. 0.25 m	0.5 points/m^2	7–15 days	Medium
Topographic LiDAR[c]	0.15–0.25 m	25 points/m^2	7–15 days	Medium
RC-APP[d]	Up to 0.025 m	100 points/m^2	<3 days	High
Classic surveying[e]	Impossible	Limited by operator	10–15 days	Medium–low

[a] Satellite data by Synthetic Aperture Radar (SAR). Since the cost of Interferometric Synthetic Aperture Radar (InSAR) data is higher than SAR data, InSAR technique is not considerated.
[b] LiDAR data aboard aircraft.
[c] Topographic LiDAR aboard helicopter.
[d] Proposed technique.
[e] GNSS – kinematic.
[f] GSD: ground sample distance (pixel size on the ground).

double than for areas greater than 648 km^2, being an inefficient technique for reduced study areas of few km^2. As regards classic surveying, allows a good vertical uncertainty (Molina et al., 2014), however the altimetric spatial resolution is affected by operator expertise. This is an important disadvantage because an insufficient number of measured points and/or badly distributed will affect the inundation area definition, as well as the generation of a robust and continuous geometric model of the river. Furthermore it does not allow obtaining an orthophotos either. Classic surveying would be a suitable technique for small extension study cases studies. Finally, the proposed technique can achieve better spatial resolution and higher density of points than other techniques. Moreover, a significant reduction in costs is achieved, because the mobilization costs are approximately ten times less than techniques such as LiDAR as well as the others cost elements (flight operator, tandem trike renting, flight insurance, planning and flight).

RC-APP comprises a manned aerial platform (tandem trike, ULM type) equipped with a navigation system and gyro-stabilized cameras platform MUSAS®. The MUSAS® system guarantees the orientation of the camera according to flight planning. Both platforms, air and gyro-stabilized, constitute an innovative alternative to airplanes and satellites in the acquisition of geospatial information, in the range proximal remote sensing, to integrate into a single aerial platform, remote sensing and photogrammetry, with the advantages of obtaining a high spatial resolution and accuracy.

As regards the UAV, the proposed procedure avoids the limitations of autonomy of these systems (Hardin and Jensen, 2011). The technical specifications of the aerial platform and system gyro-stabilized are detailed in Ortega-Terol et al. (2014).

To get the defined restrictions of spatial resolution is necessary rigorous flight planning, which will determine the choice of camera lens and flight parameters. The planning and execution of flight was carried out with MFlip software (Hernandez-Lopez et al., 2013) taking into account the overlap between images and GSD variation due to terrain, as well as estimated errors of aircraft positioning.

The camera selection was made according to the specifications of the sensor, due to their better dynamic range and higher pixel size. In addition to these factors, the performance of the lens used must be considered. As regards the focal length was chosen for the final compromise between spatial resolution and covered area, taking into account the Spanish legal provisions on the maximum height of flight for the type of aircraft (Table 2).

On the other hand, it should not be overlooked that the photogrammetric model should be geo-referenced to the legal system coordinates of the area, UTM 30N ETRS89 (EPSG 25830) by Ground Control Points (GCP), and it should be identifiable on the ground

Table 2
Camera, technical specifications and flight height.

Camera. Technical specifications			
Sensor type			CMOS
Sensor size			36 × 24 mm
Resolution (effective pixels)			21.1 Mp
Image size			5616 × 3744 pixels
Pixel density			1.5 Mp/cm^2
Pixel size			6.41 × 10^{-3} mm
Radiometric resolution			14 bits
Focal length			50 mm
Flight height			
	150 m	200 m	300 m
GSD (m)	0.019	0.026	0.038
Cover area (m)	107 × 71	146 × 97	213 × 142

and on the images. For that, it has been used a Global Navigation Satellite System (GNSS) observation, with a bi-frequency receiver Leica GPS1200 as rover and reference station AVIL, of the regional GNSS network (ITACyL, 2014). A total of 24 points, 10 GCP and 14 check points were observed, these latter for geometric control and accuracy assessment of the 3D model (Fig. 2).

4.2. Stage-2. Photogrammetric processing

At this stage, 3D geometric riverbed model reconstruction takes place through photogrammetry. It is an important phase of the study, because the errors generated in the 3D model is fully transmitted to the hydraulic simulation, which should address in a rigorous way to reduce the error of the geometric model, and improving the following hydraulic analysis (stage 4) (see Fig. 3).

At present, the photogrammetric processing has experienced significant progress thanks to the SfM techniques, Structure from Motion (Agarwal et al., 2009; Snavely et al., 2010). These are based on the principle of epipolar geometry (Hartley and Zisserman, 2004) to recover the 3D geometry of a scene or object captured from uncalibrated cameras, through the calculation of the fundamental matrix (Luong, 1992; Luong and Faugeras, 1996), which is based on the essential matrix (Longuet-Higgins, 1981).

Under this new approach of processing and in order to automate and facilitate the workflow, several software (commercial and open source) have been developed This is an advantage since allowing researchers and engineers process their own dataset and consequently, it is possible to speed up the decision making process by reducing the number of people involved. However, this ease of use has the disadvantage of the lack of details on the generation of processing and the internal model (Cramer et al., 2013). Therefore, the planning evaluation and accuracy in data

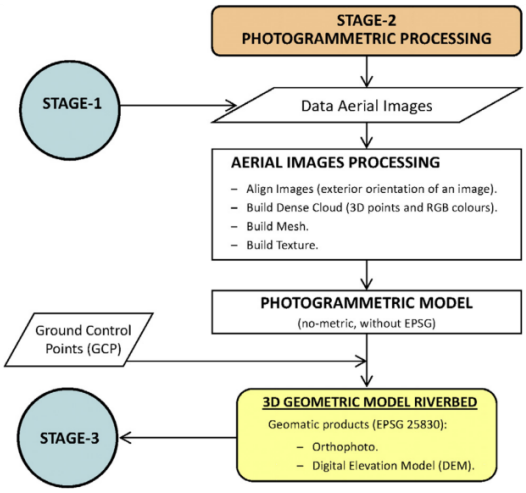

Fig. 3. Processing scheme.

acquisition is a critical issue to ensure the quality of the final 3D model.

In today's digital context, it cannot be ignored that the processing time increases exponentially with the number of images (Rieke-Zapp and Nearing, 2005). Therefore it is necessary to optimize the processing time through approximate knowledge of the external orientation of the flight cameras. This took place by the mono-frequency GNSS equipment on board the airborne platform because the positioning error is not significant compared to the flight baseline, or distance between fotocenters.

The 3D model generation took place through software PIX4D Mapper®. The operation of matching between images is solved by the descriptor DAISY, very efficient for computing dense models (Tola et al., 2010) because it uses a circular grid due to its better location than the rectangular one (Mikolajczyk and Schmid, 2005).

In the process, the phase of geo-referenced 3D model legal system coordinates of the area is crucial, UTM 30N ETRS89 (EPSG 25830), using GCP of the GNSS observation. These were chosen considering their spatial distribution, and applying to them the criterion 3 sigma for acceptance of points (Nkurunziza and Vermeire, 2014). Table 3 shows the errors obtained for the riverbed 3D model.

4.3. Stage-3. Geometric model

A correct modeling of floods over a terrain must be based, first, on the construction of a continuous, accurate and robust geometric model, which correctly synthesizes the riverbed. Furthermore, the bed channel has been more carefully studied according to the inundated area for the 10 years Return Period (RP) (high probability scenarios), according to the National System of Flood Zone Mapping (SNCZI) (MAGRAMA, 2011).

Since it determines the validity of fluvial 3D geometric model obtained in processing, this Stage-3 is crucial in the proposed methodology. The decision of using the 3D model for the construction of geometric model of the hydraulic simulations is made through the verification and determination of the 3D model accuracy.

The National Plan for Territory Observation (PNOT) (IGN, 2014), and the application of directive INSPIRE, Infrastructure for Spatial Information in the European Community (MFOM, 2014), allows getting digital aerial orthophotos with resolution of 25 or 50 cm and LiDAR DEM, at ground level (RMSE ± 0.50 m), with initial density 0.5 points/m^2 and update period of 2–3 years (IGN, 2014), through the National Plan of Aerial Orthophotography (PNOA).

This level of cartographic development allows a double verification by (1) LiDAR flight of the study area, and (2) check points. It should be noted that in Spain LiDAR flight PNOA is the fundamental geometric basis of SNCZI (MAGRAMA, 2011) to obtain from the National Center for Geographic Information (CNIG, 2014).

4.3.1. LiDAR Verification

Fig. 4 shows the checking of the detail technique applied in the representation of the topography of the riverbed against which can be obtained with LiDAR technology.

4.3.2. Check points verification

By means of check points, or ground truth, obtained in the GNSS observation, altimetry 3D model accuracy is evaluated. The geometric accuracy data is relevant to support the decision making because it influences directly the reliability of the results of the hydraulic simulations and modeling of floods.

The determination of the accuracy of the 3D model takes place from a metrological point of view, through an evaluation of the type A uncertainty altimetry, obtained from a probability density function derived from an observed frequency distribution, according with point 4.2 of (CEM, 2008).

The accuracy of the 3D model is determined by the differences between the surface of the RC-APP and the surface of verification by check points. Theoretically, instrumental errors, typical of survey observations as GNSS observation, follow normal distributions as it is shown in (Montgomery and Runger, 2006). In order to check this hypothesis, different normality tests such, as the nonparametric Shapiro–Wilk test, for its robustness, and Q–Q Plot graphical test (Table 4, Fig. 5) have been applied.

Regarding the evaluation type A, and according to the following assumptions (a) they have been made n independent observations of an input variable, (b) under the same conditions of measurement, and (c) the measurement process has enough resolution, it is possible to observe a dispersion of the obtained values, which is used as a measure of uncertainty.

Table 3
Results processed with PIX4D Mapper®.

Processing PIX4D Mapper®				
Summary	Camera name	Canon EOS 5D Mark II		
	Average ground sampling distance (GSD)	2.29 cm		
	Images	Median of 78292 points per image		
	Matching quality	Median of 43997.2 matches per calibrated image		
Bundle block adjustment	Number of 2D/3D keypoint: observations	7529622/2502589		
	Mean reprojection error	0.33 [pixels]		
Ground Control Points (GCP)		Error X[m]	Error Y[m]	Error Z[m]
	Mean	−0.0051	0.0064	0.0185
	RMS error	0.0858	0.1043	0.0667

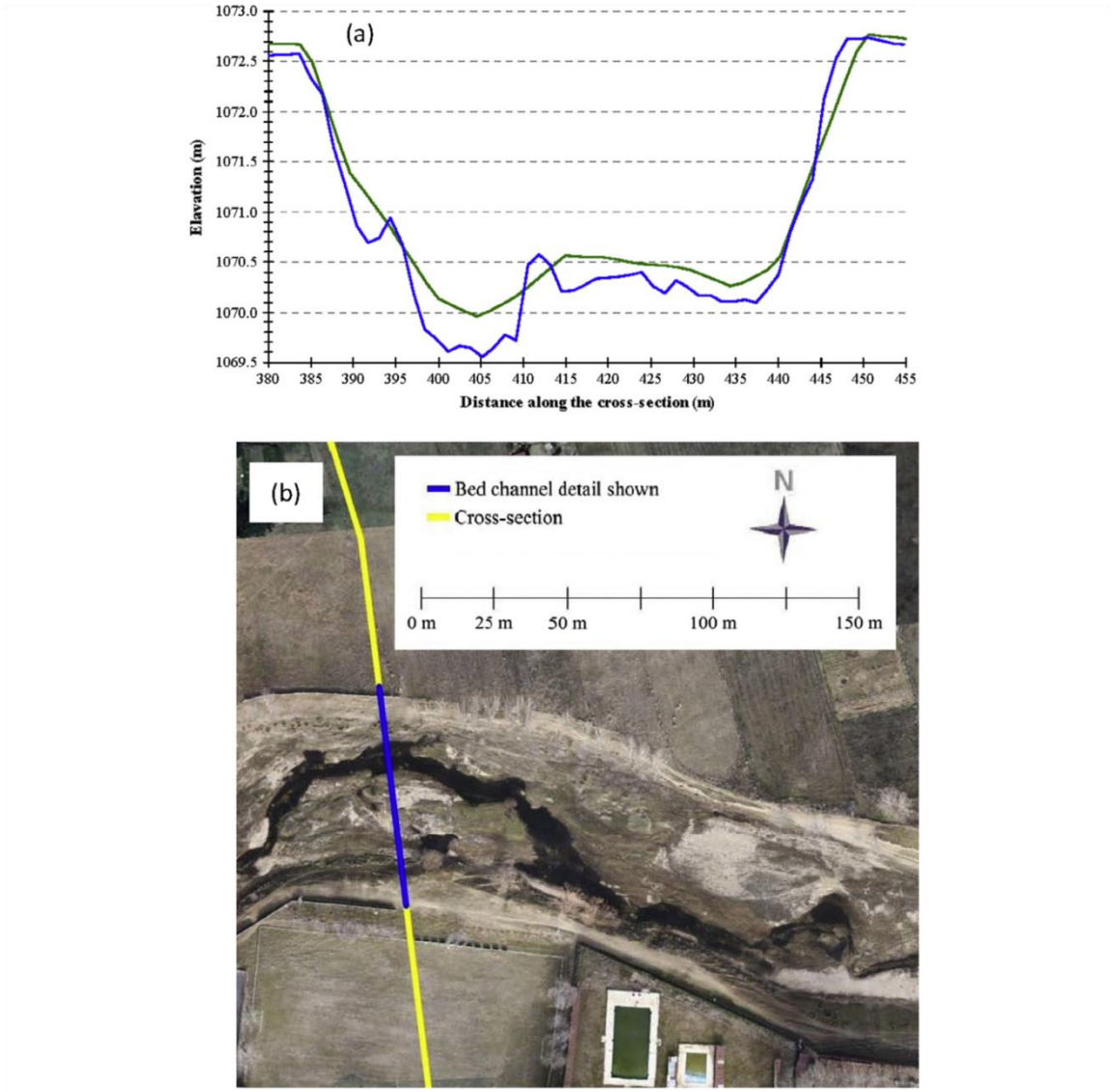

Fig. 4. LiDAR Verification river channel. S-1 cross-section of the study. (a) S-1 cross-section of the study. Blue cross-section: ground RC-APP DEM. Green cross-section: ground LiDAR DEM. (b) Aerial view of detail of the cross-section (2.5 cm orthophoto). (For interpretation of the references to color in this figure legend, the reader is referred to the web version of this article.)

Table 4
Statistics and normality test.

Statistics. Differences RC-APP DEM variable			
Differences RC-APP DEM	*N* valid/missing	Mean	Std. deviation
	14/0	−0.0234	0.1008
Test of normality: Shapiro–Wilk			
Differences RC-APP DEM	Statistic	*n*	*p*-value
	0.981	14	0.981

In this sense, the best estimate of the expectation mathematical of a random variable is the arithmetic mean $\bar{q}$ of the n values observed $q_j (j = 1, 2, \ldots, n)$ Eq. (1). Moreover, the values of individual observations q_j differ due to random effects; therefore the variance $\sigma^2(q)$ of the probability distribution of input variable is estimated through the experimental variance $s^2(q)$ of the q_j observations Eq. (2). The variability of the observed values q_j, named the experimental standard deviation, is obtained by positive square root of the experimental variance $s^2(q)$.

Since the variance of the arithmetic mean is suitably estimated by experimental variance of the arithmetic mean $s^2(\bar{q})$ Eq. (3), according to (CEM, 2008), the experimental variance of the arithmetic mean $s^2(\bar{q})$ and the experimental standard deviation of the arithmetic mean $s(\bar{q})$ (positive square root of $s^2(\bar{q})$), quantify how well the arithmetic mean $\bar{q}$ estimates the expectation mathematical

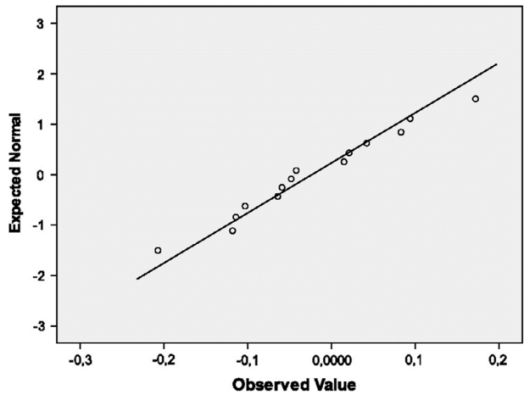

Fig. 5. Q–Q plot for normality assessment.

of an input variable. Therefore, it is possible measure of the uncertainty of $\bar{q}$ by the standard uncertainty u Eq. (4).

On the other hand, since geometric data from two different sources, GNSS observation and RC-APP model have been used, the experimental standard deviation of the arithmetic mean and the uncertainty must be reformulated according to Eqs. (5) and (6) respectively. In Eq. (5), $\sigma_{z_{GNSS}}$ is the altimetric precision of the check points utilized (average of their altimetry precision), and $\sigma_{z_{RC\text{-}APP}}$ is the altimetric precision, of RC-APP model (standard deviation of the differences between the surface of the RC-APP and the surface of verification by check points). Lastly, the model accuracy RC-APP is obtained by Eq. (6).

$$\bar{q} = \frac{1}{n}\sum_{j=1}^{n} q_j \tag{1}$$

$$\sigma^2(q) = s^2(q) = \frac{1}{n-1}\sum_{j=1}^{n}(q_j - \bar{q})^2 \tag{2}$$

$$s^2(\bar{q}) = \frac{s^2(q)}{n} \tag{3}$$

$$u = \frac{s(\bar{q})}{\sqrt{n}} \tag{4}$$

$$s(\bar{q}) = \sigma_{\varepsilon_i} = \sqrt{(\sigma z_{GNSS})^2 + (\sigma z_{RC\text{-}APP})^2} \tag{5}$$

$$u_A = \frac{\sigma\varepsilon_i}{\sqrt{n}} \tag{6}$$

Table 5 shows the result of model accuracy RC-APP.

Therefore, the accuracy of RC-APP model, by evaluation type A, is (-0.02 ± 0.03) m.

4.3.3. Geometric model

Nowadays, GIS tools are indispensable for geospatial information analysis, such as DEMs or digital aerial orthophotos. Firstly, it has been built riverbed geometric models through GIS software, LiDAR and RC-APP, performing strategically, and in the same places, the channel cross sections in both models, and determining the relative distances between sections. Secondly, the cross sections of the model LiDAR have been used in the LiDAR Verification (Figs. 2 and 4).

On the other hand, it should not be overlooked that a high density of points (about 100 points/m^2) has important effects in the construction of geometric model, such as (a) more detail of the cross section, which improves the knowledge of the hydraulic variables in natural waterways, (b) it is not necessary to use GIS simulation models for cross section definition that would imply a digitization, which bring uncertainty in its definition, and (c) it is not required processing point cloud (in the case of a low points density), which is other source of uncertainty, all these make more efficient the methodology used.

Table 5
Model accuracy RC-APP DEM.

Check points (ground truth)		RC-APP DEM	
N	14	*N*	14
Error of mean (m)	0.012	Error of mean (m)	−0.02
A priori error, precision (m)	0.012	*A priori error*, precision (m)	0.10
A posteriori, accuracy (m)		*A posteriori*, accuracy (m)	0.10
		u_A (m)	0.03

4.4. Stage-4. Hydraulic processing

This represents the last stage of the research. It comprises the hydraulic simulations, according to the scenarios of occurrence probability under European legislation (EU Directive, 2007) and Spanish (Ministerio de la Presidencia, 2010): (a) low or extreme events (RP 500 years), delimitation of the flood zone, (b) average (RP $\geqslant$ 100 years) materializing the Preferential Flow Area, and (c) high (Return Period 10 years), and using the 3D riverbed geometric models, LiDAR and RC-APP (Table 6).

The hydraulic simulations cannot be separated from its spatial component. In this respect, the watershed, as territorial unity, is the set of water realities through the natural drainage network, which converge at a point where natural flows are evaluated in the analyzed stretch (X = 351828 m, Y = 4497706 m, EPSG25830), determining a watershed of 530 km^2 and defining a concentration time of 11.7 h, depending on the main channel length (39.9 km) and range of altitudes (between 1500 m a.s.l and 1070 m a.s.l).

On the other hand, the watershed behavior is evidenced through the water flow. Hydrological conditions, basic hydraulic parameters, along with the reduction of transport capacity of the watercourse and modification of the natural conditions of basin runoff (anthropogenic factors) are, among others, the causes that make the existence of flooding.

However, this study is approached from a geomatic point of view, where the water flow, understood as the product of section (depending on the depth) by the speed (depending on the hydraulic radius depending on the section), is eminently a geometrical product. Consequently, within this geomatic context it was not considered a specific rainfall–runoff model. This would have involved taking into account the random component of rain and/or the study of equiprobable series, for the definition of rainfall patterns, and getting the water flows to the hydraulic simulations with a certain degree of uncertainty. This is to be made for forthcoming investigations.

In this sense, the hydrological study is addressed through maximum discharges series, relating the magnitude of peak flood flow with its annual probability of occurrence or RP (quantile), which is essentially a statistical problem.

Table 6
Geomatic products used in hydraulic simulations.

Geomatics products		LiDAR (PNOA)	RC-APP
Orthophoto	Resolution (GSD)	0.25 m	0.025 m
	Time reference	2010–2011	2013/12/13
Digital Elevation Model (DEM)	Initial density	0.5 points/m^2	Approx 100 points/m^2
	Output planimetric	GRID 5 × 5 m	GRID 0.10 × 0.10 m
	Output altimetric	RMSE: ±0.50 m	Accuracy: ±0.10 m

Data gauging of peak flows are adjusted to a distribution function, once a validation of quality and data consistency is carried out. Three different Return Periods (RPs) of 10, 100 and 500 years have been selected, corresponding to the stage of high, medium and low probability of the applicable legislation. Consequently, the selected quantiles are obtained at the gauged points. The adjustment of frequency is carried out through Generalized function Extreme Values (GEV), adjusted by the method of L-moments. These methods have been used in different hydrological studies such as Norbiato et al. (2007) and Yang et al. (2010).

Considering that the point of flow assessment is not a gauging station, results extrapolation is made for the quantile at that point. This extrapolation is carried out according to statistical multiple regression models that relate the quantiles of gauging stations or specific statistics with physiographic and climatic characteristics of the basin. Consequently, by knowing physiographic and climatic characteristics of the regression, quantiles can be estimated.

Water flows are provided, by the Duero river basin authority and comprise a map of instant peak flows in natural regime (CEDEX, 2013). This flows are $Q_{10} = 112\ m^3\ s^{-1}$, $Q_{100} = 229\ m^3\ s^{-1}$ y $Q_{500} = 330\ m^3\ s^{-1}$.

Regarding the construction of the hydraulic model, the existing structure (bridge) on the analyzed stretch is not modeled hydraulically. The study is focused on the study of the influence of the two considered geometric sources (innovative RC-APP vs. traditional LiDAR) in the floods modeling results. Furthermore, the study is also aimed to estimate the hydraulic parameters associated with it, and consequently, assessing the technical and methodological suitability for application to Hydraulic Studies, river engineering and risk assessment flood.

HEC-RAS® software, has been used because simplification in the calculation of flood wave propagation in 1D flow, is suitable for the geomatic field of study. The simulations are performed under a mathematical model with fixed river bed channel, non-erodible without accretion, based on establishing the continuity equation and energy between two sections of the riverbed, considering the constant flow as steady state (Martínez Marín, 2001). In forthcoming studies further elements will be incorporated and 2D flow conventional softwares, such as MIKE21

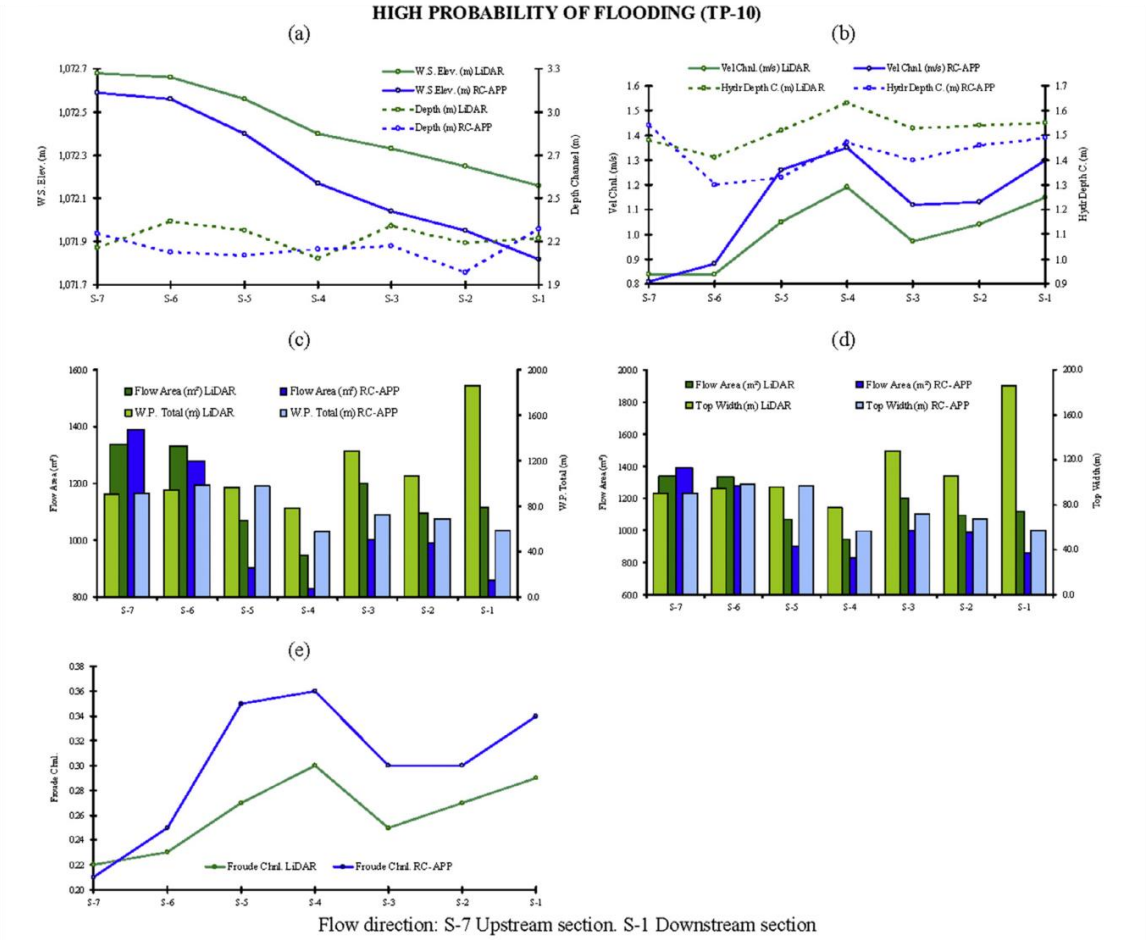

Fig. 6. High probability of flooding. Hydraulic parameters. (a) Water surface and depth in the central channel, (b) speed and hydraulic radius in the center channel, (c) area and perimeter wet, (d) wet area and free surface of the fluid and (e) Froude number.

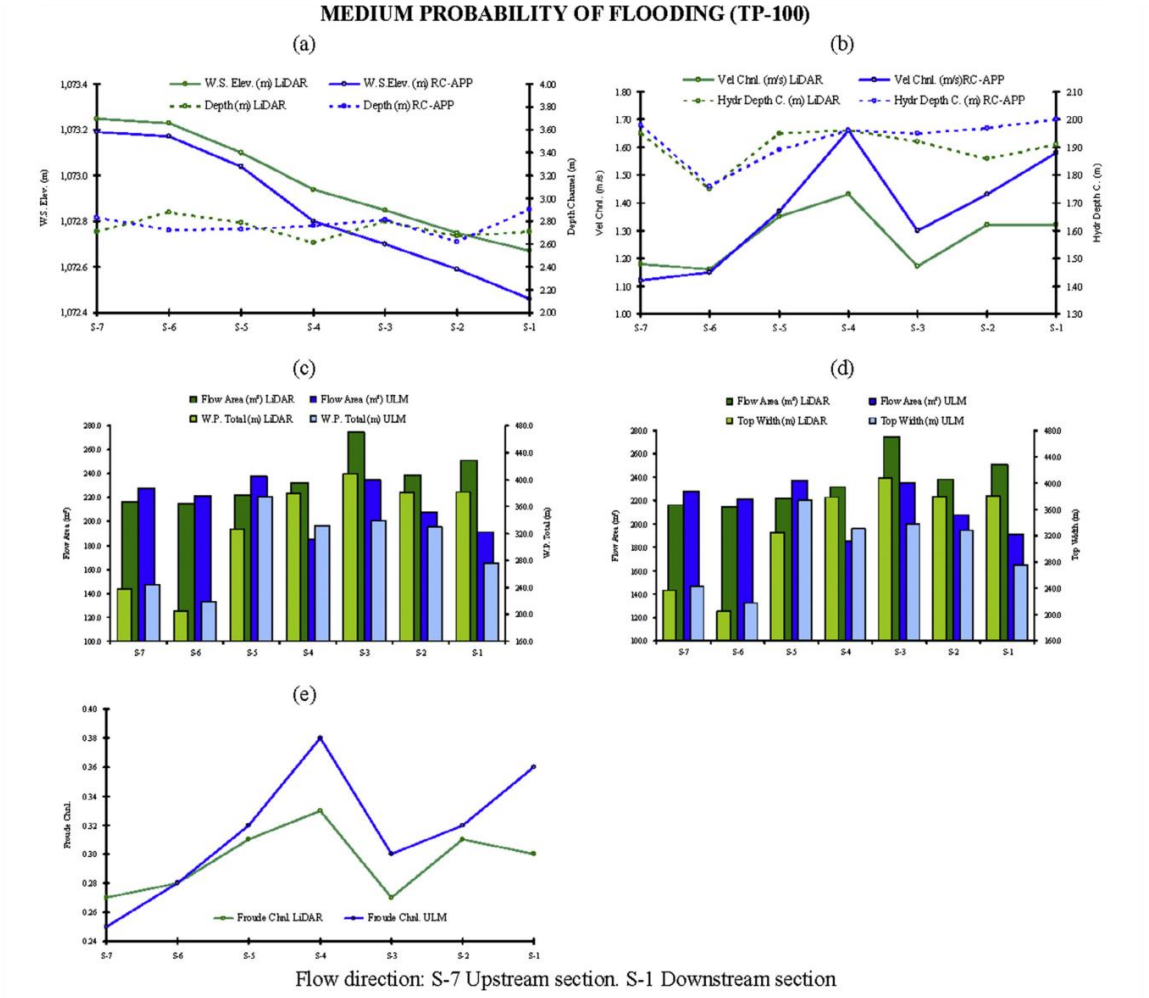

Fig. 7. Medium probability of flooding. Hydraulic parameters. (a) Water surface and depth in the central channel, (b) speed and hydraulic radius in the center channel, (c) area and perimeter wet, (d) wet area and free surface of the fluid and (e) Froude number.

(Warren and Bach, 1992) or latest, such as IBER (Blade et al., 2014), will be used according to the results in studies such as Horritt and Bates (2002) and Tsakiris (2014). Furthermore, a specific hydrological study to define the flows in the study area will be performed as well.

Given this situation, two hydraulic simulations were carried out, in which the hydraulic parameters are unique, varying only the DEM (cross section) and the boundary conditions associated with it (normal hydraulic depth). Given the geometrical context, average values for roughness coefficient (n) were adopted according to US Army Corps of Engineers (2010), so that the simulations reflect reality in the area ($n = 0.006$ for tree-covered, $n = 0.045$ main channel). Finally, once executed simulations, Flood Maps and desired hydraulic parameters are generated through the GIS tool, for the process of decision making in the river field. The hydraulic model was calibrated with the hydraulic depth values and water flows taken at the Gauge Station Ávila (code number 2046) located 5.5 km downstream the studied river stretch.

Under this approach, the differences in flood conditions and hydraulic outcomes must be produced, exclusively, due to the influence of the 3D model river geometry.

5. Results

5.1. Influence of geometry on hydraulic parameters

Typical hydraulic free regime parameters in open channels and rivers, such as the Froude number (F) or influence of weight, speed, wetted perimeter-section, hydraulic radius or average value of shear stress per section, among others, have in common that they are determined by geometric parameters, so an accurate and detailed geometry of the channel will result in a better understanding of them and hydraulic systems.

The influence of geometry is limited to the cases of high and medium probability, because for a low probability (RP-500), the

water flow is obtained by a rating curve, where information is often not available upstream and may not produce a valid water flow value. For the case of RP-500 years, the effect of a wide and homogeneous flood plain in the attenuation of the flood wave it has been highlighted. In this sense, it has been observed, that only increase the purely geometric hydraulic parameters due to the increased elevation of the water surface. Consequently, the variation of the rest of the parameters is not significant, compared to those obtained from the simulation of RP-100 flow.

In Figs. 6 and 7, a comparative analysis of the main hydraulic variables obtained through the two DEMs, RC-APP and LiDAR, is carried out for scenarios of high and medium probability.

In Graphic a, of Figs. 6 and 7, it is seen that the larger detail from RC-APP section and the difference between both models implies a higher water surface elevation for LiDAR model than for RC-APP model. The most pronounced discrepancy is in the case of RP-10, due to the effect of larger detail in the RC-APP model. The influence between both terrains, due to the accuracy of 3D models as well as to a greater topographical detail, is evident in the hydraulic depth; which is significantly lower in the RC-APP model, leading to a lower water surface elevation. Furthermore, the best definition of the wet section provides a better knowledge of the velocity at the center channel, Graphics b and c, Figs. 6 and 7.

The positive effects of a better riverbed geometric definition are more evident in the case of water flow RP-10, c and d Graphic Fig. 6. As consequence of that, both the section and the wetted perimeter are significantly lower in the RC-APP model than in the LiDAR model. This provides a substantial difference in the inundated area of the free water surface, and therefore, the flooding modeling (Sections S-3, S-2, especially S-1). This is especially interesting when defining and limiting the susceptible areas to flooding. In this sense, in Fig. 8, it is shown that the more detailed and the less uncertainty model RC-APP provides the lower inundated area modeling of floods. This has important implications for the assessment of exposure to the risk to flooding.

The effects of a more detailed RC-APP model against the LiDAR model are clearly evidenced itself, if they are globally analyzed for the entire stretch (390 m). Those effects can be evidenced on the, strictly hydraulic geometrical parameters and those, derived from them:

- Flow area: An increase of 10% is produced in the LiDAR section for water flow RP-10 (116 and 104 m^2). The same trend is maintained in the case of flow RP-100, where the increase is about 9% (236 and 215 m^2).
- Wetted perimeter: The difference reaches 30% (112 and 78 m), LiDAR section higher than RC-APP section, in the flow RP-10, and in the case of RP-100 is 9% (331 and 302 m).
- Top width wetted cross section: The difference in inundated area water flow for the RP-10 is 31% (111 and 77 m) higher in LiDAR section, in water flow RP-100 the discrepancy is 9% (331 and 301 m).
- Average velocity of flow in main channel: The lower section of the RC-APP model increases speed by 11% for RP-10, and 8% with RP-100.
- Hydraulic depth in channel: The geometric influence is reduced to only 2% for the flow T-100, and 6% for water flow T-10. Both with higher value in the LiDAR section than in the RC-APP section.
- Froude number for the main channel: The difference reaches 15%, the water flow RP-10, and 7% in the case of RP-100. With both water flows, this parameter is lower in the LiDAR section, which provides uncertainty when it comes to assessing the stream regime.

5.2. Influence of geometry on the simulation modeling

As it has been already proven, the geometric accuracy affects directly on the hydraulic variables and, consequently on the modeling and identification of susceptible areas to flooding (Figs. 8 and 9). Therefore, an accurate representation of relief and minimal uncertainty of 3D reference model are determining factors.

In Table 7, inundated area surfaces associated with the established water flows probability scenarios are indicated, according to the DEM used in each hydraulic simulation.

For high probability, the average difference is relevant (0.22 m) for the water surface elevation. This is because of the more detailed model and less elevation of the RC-APP model. This demonstrates the positive influence of the detail degree on the representation of riverbed central channel, through the applied technique-methodology.

On the other hand, the central channel geometry has sufficient transport capacity for the considered water flow, implying that there is no practically an impact on the modeling of floods. In this case, the RC-APP model shows a lower inundated area. Due to the section transport capacity, the influence of geometric accuracy has no significant effect on the modeling of floods. However, the model accuracy LiDAR causes that the inundated area is 4.4% higher than it would have been with the RC-APP model.

In the case of medium probability, on a stretch of just 390 m, the inundated area by LiDAR model is higher than inundated area by RC-APP model about 29,250 m^2. This involves 21.5% more inundated area for an average difference in the surface water elevation of only 0.12 m between both 3D models.

Regarding the low occurrence probability, the higher inundated area from LiDAR model is maintained. This inundated area through LiDAR implies an absolute difference of 5600 m^2 (3.7%), for an average difference between surface water of only 0.10 m. In this sense, the existence of a difference of 5600 m^2 in the inundated area is still relevant, because it is common, for this type of flooding, that a small different in inundated area cause serious damage.

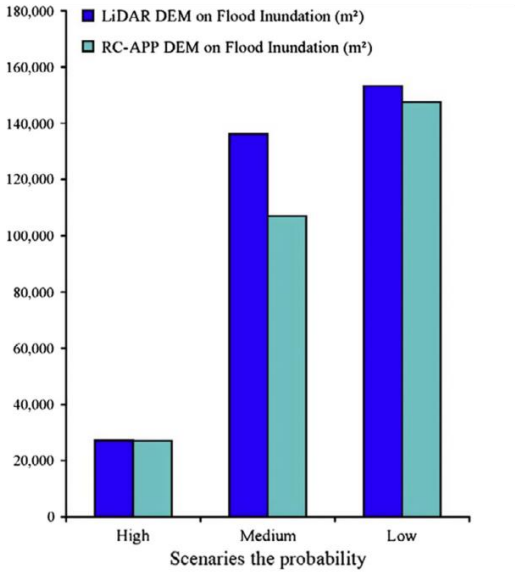

Fig. 8. Effect of RC-APP and LiDAR DEM on flood inundation under European legislation (EU Directive, 2007) and Spanish (Ministerio de la Presidencia, 2010).

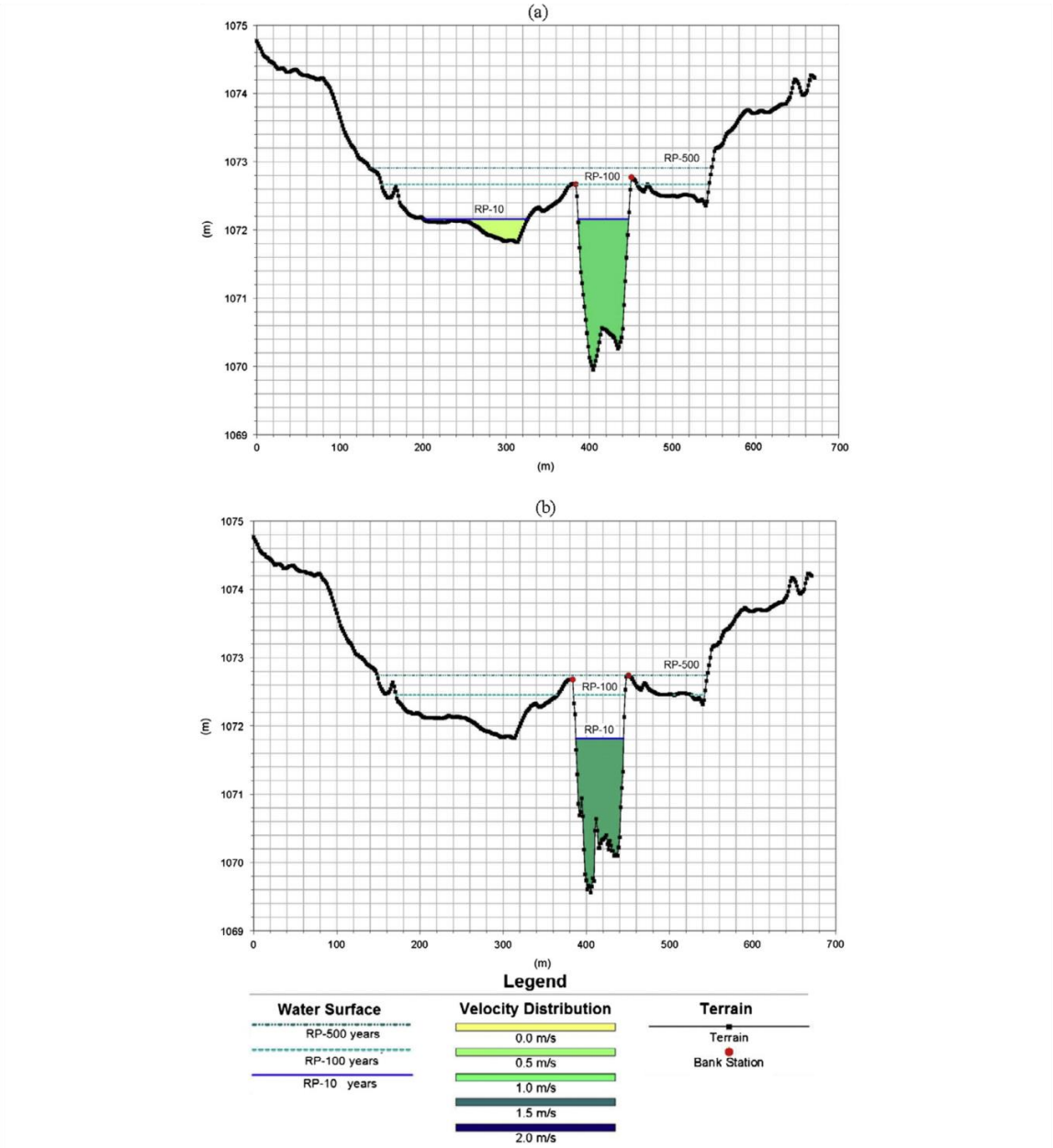

Fig. 9. Simulation results. S-1 cross-section. Vertical axis represents water surface elevation (m), and horizontal axis represents distance along the cross-section (m). Manning $n = 0.045$ in all cross-section. (a) LiDAR DEM. (b) RC-APP DEM.

Table 7
Effects of geomatic products on inundation map.

Geomatics products – flood modeling (m^2)		
Probability scenarios	Traditional (LiDAR DEM)	Innovative (RC-APP DEM)
High (RP-10)	27,200	27,050
Medium (RP-100)	136,250	107,000
Low (RP-500)	153,200	147,600

Moreover, this higher surface area can lead to an unnecessary increase of the risk level.

In order to summarize, for this case study, results on inundated area from LiDAR model area are larger than those obtained through RC-APP model. Thus, LiDAR model might produce an overestimation of the water surface (see Casas et al., 2006).

Fig. 10 shows the influence of the different models (RC-APP and LiDAR) on the flood inundation.

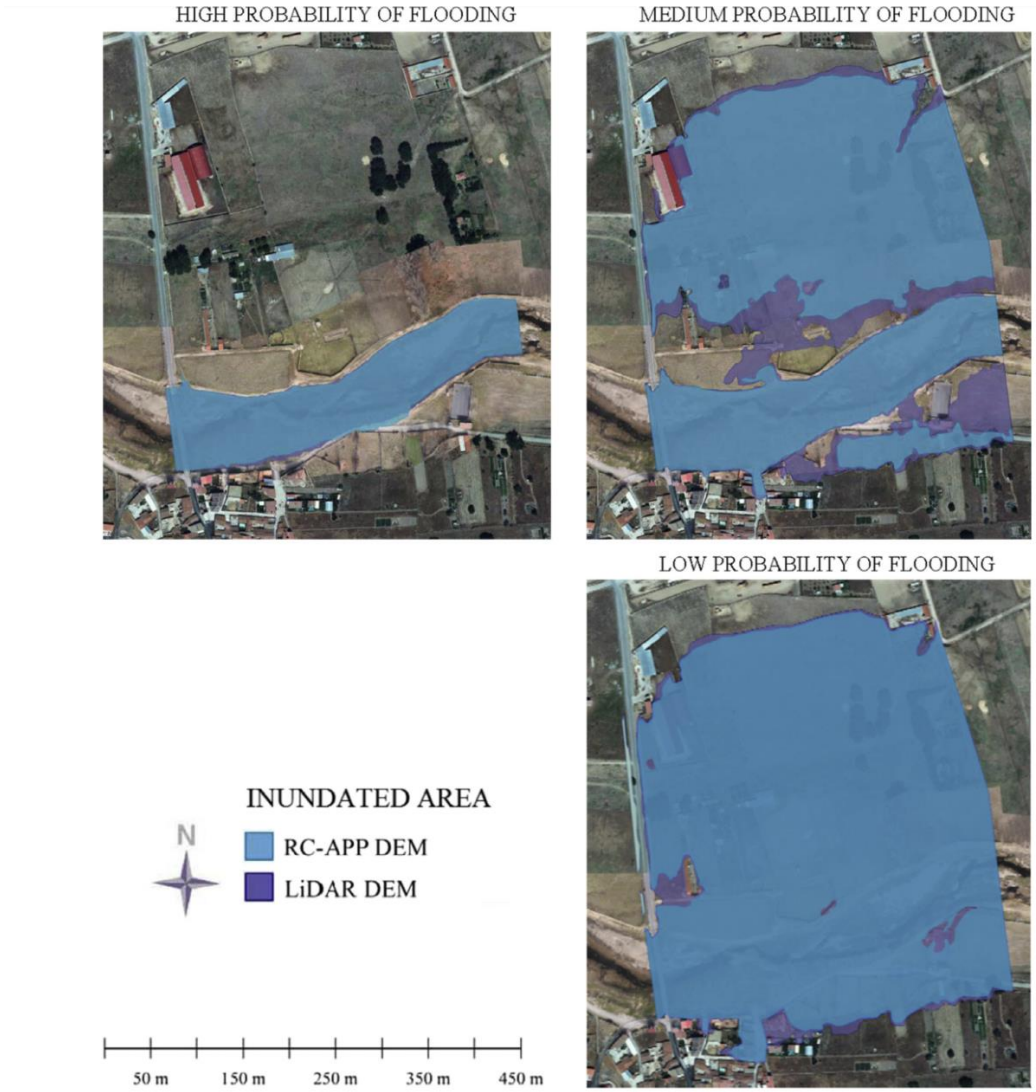

Fig. 10. Map flood modeling, with RC-APP and LiDAR DEMs, under European legislation (EU Directive, 2007) and Spanish (Ministerio de la Presidencia, 2010).

6. Discussion and conclusions

In the modeling and analysis of flooding, the relationship between flow and terrain is inseparable. On the other hand, the hydrological behavior of a basin is characterized by randomness, in magnitude and occurrence of events. Extreme events are increasing in frequency and magnitude, partly due to the phenomenon of climate change. It is therefore, necessary for the society to adapt to these new hydrological realities in the most efficient way (time-cost).

This adaptation must be articulated on a decision making process of and based on optimal design of technical solutions. Here, the geometric component is essential, not only as a cartographic support, but also as a component that reduce uncertainty in the process. In this sense, it is necessary to work with efficient and accurate methodologies for representing 3D fluvial geometric model.

All that technical methodology, applied in this study, offers important advantages in geomatic component, modeling and analyzing risk flood. First, it is possible to have a continuous geometric 3D riverbed model, with an accuracy of (-0.02 ± 0.03) m. This involves one magnitude order higher than the traditional and conventional techniques such as LiDAR (RMSE ± 0.50 m). Furthermore, good results of LiDAR technology (Cook and Merwade, 2009), have been improved significantly through RC-APP.

For a medium probability of flooding, the difference between 3D models in the definition of the average water surface elevation is about 0.12 m that represents a difference of 29,250 m^2. This involves a 21.5% increase in inundated area in the case of model LiDAR. This difference is significant in assessing the risk of floods.

It has been checked, in the three considered probability scenarios, that the inundated areas obtained by the RC-APP model are lower than those obtained when using the LiDAR model. These results are due to the high density of points in addition to the accuracy the RC-APP data compared to LiDAR data. The decreasing trend in inundated area when are employed more accurate geometric models, is described in (Casas et al., 2006), is maintained with RC-APP.

As it was seen through the manuscript, the RC-APP technique has favorable effects when it is applied to areas of high exposure to floods, it is allows the risk level as a consequence of a more faithful representation.

Regarding the hydraulic variables, RC-APP technical-methodology has allowed a better understanding of them. For RP-10 (high probability) there is a decrease of 30% in the variables wetter perimeter, top width wetted cross section. For RP-100 (medium probability), the decrease is about 10% in the same variables. With high water flows, the influence of a wide and regular floodplain has produced only significant changes in the purely geometric hydraulic parameters. On the contrary, the hydraulic parameters derived from these they do not have relevant modifications. However, when dealing with low water flow, greater detail in the representation of the riverbed has a positive effect, which produces significant changes in the geometric hydraulic parameters strictly and those derived from them.

3D geometric model reconstructed presents the important feature of data homogeneity, being obtained from a single geometric source. On the other hand, problems of interpolation, integrability and combination of data, indicated in Merwade et al. (2008b), are eliminated due to the density of points in the model, which influence the precision of the results.

The resolution and high accuracy of the geomatic products obtained in Stage-2, allow better risk assessment and knowledge flow. This has a significant economic advantage in decision-making and the definition of technical solutions in the field of river engineering. In the case of the technical characteristics of generated geomatic products (Stage-2), the orthophoto generated is between 6 and 10 times more resolution than those obtained by traditional techniques (2.5 cm and 15–25 cm). Furthermore, DEM (approx 100 points/m^2), has a density of points hard to get by the same techniques (0.5–2 points/m^2 for LiDAR embarked on aircraft and 25–40 points/m^2 in the case of topographic LiDAR using helicopters).

The ULM aerial platform used for this study offers significant advantages because it does not require airfields to operate, has a capacity of up to 110 kg, the possibility of boarding the MUSAS® platform, and a flight autonomy of up to 3.5 h. Furthermore the means employed (aircraft, camera, software) for its simplicity, may be regarded as innovative and alternative compared to traditional and commonly used.

The interest of this study, compared with traditional studies lies also at an economic level. In this sense, ULM flight platform, sensors, software and flight infrastructure provide a significant reduction in cost, especially in mobilization costs (ten times less than techniques such as LiDAR). These aspects strengthen the idea of effectiveness established as a basic premise of this study. In economics terms, will enable more efficient use of economic resources, by public administrations and private corporations. This economic-social efficiency can be realized in more adjusted designs to the reality.

Regarding the acquisition of geometric information, and as a consequence of its photogrammetric character, it should be pointed, that this technique is sensitive to the concealments, especially in areas of dense vegetation, as well as to the specific limitations of passive sensors (photographic camera) that capture energy but do not emit any radiation to take a measurement. These apparent disadvantages can be minimized, and even not be relevant, as in this study, if it is possible to coordinate the execution of ULM flight with the phenology of vegetable species existing in the analysis area (riverside vegetation and channel). Also, the fact of using an aerial platform, makes it is more exposed to the weather than traditional aircraft.

It is intended to continue the application of this technique in future research. For instance, on the evaluation of sediment transport and its influence on reducing available water storage in reservoirs and its implications for the optimal design of scour outlet of the dam, making a multitemporal analysis of riverbed change. Furthermore, elements will be incorporated to improve the hydraulic system knowledge, as the generation of a specific model of rainfall-runoff and using softwares 2D flow like MIKE21 or IBER, among others.

Furthermore, within the field of river engineering and hydraulics, and based on technical and reduced cost geomatic sensors, it will be analyzed their application to the study of the local and general erosion phenomenon, as well as the analysis, preventive control and maintenance of riverbeds existing structures may affected by erosion, scour or any other affection.

It is important to emphasize the accuracy of the RC-APP (-0.03 ± 0.02) m, which is similar to classic surveying technique, that can encourage the use of this technique in surveying large areas. This is because of the possibility of producing continuous models, with high point density and homogeneous precision, which results in the final suitably metric precision of the generated products, because of the integration of both techniques.

This technique-methodology may have another important niche application, not just in the river area as a low cost and high resolution tool, but also, for the management, control and surveillance of public water and wastewater discharges. Furthermore, is also possible to identify the particularity of the temperature by embarking a thermographic sensor.

Finally in other civil engineering fields such as the Land Transport Infrastructure, it is immediate the implementation as a tool for mapping, control and monitor the implementation of this type of linear projects.

Acknowledgments

The authors thank especially Mr. Diego Guerrero Sevilla, pilot ULM aircraft, the realization flight and fluvial acquisition data set.

This research has been partially supported by the GESINH-IMPADAPT project (CGL2013-48424-C2-2-R) of the Spanish Ministry of Economy and Competitiveness (Plan Estatal I+C+T+I 2013–2016).

References

Adams, J.C., Chandler, J.H., 2002. Evaluation of lidar and medium scale photogrammetry for detecting soft-cliff coastal change. Photogramm. Rec. 17, 405–418.

Agarwal, S., Snavely, N., Simon, I., Seitz, S.M., Szeliski, R. 2009. Building Rome in a Day. In: 2009 IEEE 12th International Conference on Computer Vision (Iccv)., pp. 72–79.

Aguilar, F.J., Mills, J.P., 2008. Accuracy assessment of lidar-derived digital elevation models. Photogramm. Rec. 23, 148–169.

Airbus Defense & Space and Infoterra SGSA. 2015 <http://www.infoterra.es/datos-satelite-precios> (Accessed 31.01.15).

Andreu, J. 1993. Conceptos y métodos para la planificación hidrológica. Capítulo 1. Reflexiones sobre la planificación hidrológica. In: Sauquillo Herraiz, A. (Ed.), Barcelona, CIMNE, Centro Internacional de Métodos Numéricos en Ingeniería, pp. 3.

Ashley, R.M., Balmforth, D.J., Saul, A.J., Blanskby, J.D., 2005. Flooding in the future – predicting climate change, risks and responses in urban areas. Water Sci. Technol. 52, 265–273.

Balairón Pérez, L. 2002. Gestión de recursos hídricos. Los recursos hídricos, Barcelona, Edicions UPC, pp. 43–68.

Bales, J.D., Wagner, C.R., 2009. Sources of uncertainty in flood inundation maps. J. Flood Risk Manage. 2, 139–147.

Bates, P.D., De Roo, A.P.J., 2000. A simple raster-based model for flood inundation simulation. J. Hydrol. 236, 54–77.

Bates, P.D., Marks, K.J., Horritt, M.S., 2003. Optimal use of high-resolution topographic data in flood inundation models. Hydrol. Process. 17, 537–557.

Bates, B.C., Kundzewicz, Z.W., Wu, S., Palutikof, J.P., 2008. Climate Change and Water. Technical Paper of the Intergovernmental Panel on Climate Change, IPCC Secretariat, Geneva, p. 210.

Biswas, A.K., Tortajada, C., 2003. An assessment of the Spanish National Hydrological Plan. Int. J. Water Resour. Dev. 19, 377–397.

Blade, E., Cea, L., Corestein, G., Escolano, E., Puertas, J., Vazquez-Cendon, E., et al. 2014. Iber – river modelling simulation tool. Revista Internacional De Metodos Numericos Para Calculo Y Diseno En Ingenieria. 30, 1–10.

Casas, A., Benito, G., Thorndycraft, V.R., Rico, M., 2006. The topographic data source of digital terrain models as a key element in the accuracy of hydraulic flood modelling. Earth Surf. Process. Landforms 31, 444–456.

CEDEX. 2013. Mapa de Caudales máximos instantáneos en régimen natural asociados a distintos periodos de retorno. CAUMAX. Marzo 2013.

CEM. 2008. Evaluación de datos de medición. Guía para expresión de la incertidumbre de medida. JCGM 2008. GUM 1995, EDICIÓN DIGITAL 1 en español (traducción 1ª Ed. Sept. 2008, original en inglés) Ed., Centro Español de Metrología CEM, pp. 12–14.

Chávez Jiménez, A. 2012. Propuesta metodológica para la identificación de medidas de adaptación al Cambio Climático en Sistemas de Recursos Hídricos. Tesis Doctoral, Universidad Politécnica de Madrid, España, 232 pp.

Chen, J., Hill, A.A., Urbano, L.D., 2009. A GIS-based model for urban flood inundation. J. Hydrol. 373, 184–192.

CNIG. 2014 <http://centrodedescargas.cnig.es/CentroDescargas> (Accessed 02.11.14).

Cook, A., Merwade, V., 2009. Effect of topographic data, geometric configuration and modeling approach on flood inundation mapping. J. Hydrol. 377, 131–142.

Cooper, H.M., Fletcher, C.H., Chen, Q., Barbee, M.M., 2013. Sea-level rise vulnerability mapping for adaptation decisions using LiDAR DEMs. Prog. Phys. Geogr. 37, 745–766.

Cramer, M., Haala, N., Rothermel, M., Leinss, B., Fritsch, D., 2013. UAV@LGL – pilot study of the use of UAV for national mapping in Germany. Photogrammetrie Fernerkundung Geoinformation., 495–509

Dawson, R.J., Hall, J.W., Bates, P.D., Nicholls, R.J., 2005. Quantified analysis of the probability of flooding in the thames estuary under imaginable worst-case sea level rise scenarios. Int. J. Water Resour. Dev. 21, 577–591.

Escuder-Bueno, I., Castillo-Rodriguez, J.T., Zechner, S., Joebstl, C., Perales-Momparler, S., Petaccia, G., 2012. A quantitative flood risk analysis methodology for urban areas with integration of social research data. Nat. Hazards Earth Syst. Sci. 12, 2843–2863.

Estrela, T., Perez-Martin, M.A., Vargas, E., 2012. Impacts of climate change on water resources in Spain. Hydrol. Sci. J.-J. Des Sci. Hydrologiques 57, 1154–1167.

EU Directive. 2007. EU directive of the European parliament and the european council on the assessment and management of flood risks. (2007/60/EU).

Garcia-Pintado, J., Neal, J.C., Mason, D.C., Dance, S.L., Bates, P.D., 2013. Scheduling satellite-based SAR acquisition for sequential assimilation of water level observations into flood modelling. J. Hydrol. 495, 252–266.

Gonzalez-Aguilera, D., Gomez-Lahoz, J., 2008. From 2D to 3D through modelling based on a single image. Photogramm. Rec. 23, 208–227.

Hardin, P.J., Jensen, R.R., 2011. Small-scale unmanned aerial vehicles in environmental remote sensing: challenges and opportunities. Gisci. Remote Sensing 48, 99–111.

Hartley, R., Zisserman, A., 2004. Multiple View Geometry in Computer Vision, second ed. Cambridge University Press.

Haugerud, R. 2009. Buying LiDAR data. In: Geological Society of America Annual Meeting, 18–21 October 2009 Portland, Oregon, USA.

Hernandez-Lopez, D., Felipe-Garcia, B., Gonzalez-Aguilera, D., Arias-Perez, B., 2013. An automatic approach to UAV flight planning and control for photogrammetric applications: a test case in the Asturias region (Spain). Photogramm. Eng. Remote Sensing 79, 87–98.

Hodgson, M.E., Jensen, J., Raber, G., Tullis, J., Davis, B.A., Thompson, G., et al., 2005. An evaluation of lidar-derived elevation and terrain slope in leaf-off conditions. Photogramm. Eng. Remote Sensing 71, 817–823.

Horritt, M.S., Bates, P.D., 2001. Effects of spatial resolution on a raster based model of flood flow. J. Hydrol. 253, 239–249.

Horritt, M.S., Bates, P.D., 2002. Evaluation of 1D and 2D numerical models for predicting river flood inundation. J. Hydrol. 268, 87–99.

IGN, 2014 <http://www.ign.es/PNOA/presentacion.html> (Accessed 28.10.14).

Irish, J.L., White, T.E., 1998. Coastal engineering applications of high-resolution lidar bathymetry. Coast. Eng. 35, 47–71.

ITACyL. 2014 <www.itacyl.es/opencms_wf/opencms/informacion_al_ciudadano/wms/AccesoDatos/index.html> (Accessed 25.10.14).

Jung, Y., Merwade, V., 2012. Uncertainty quantification in flood inundation mapping using generalized likelihood uncertainty estimate and sensitivity analysis. J. Hydrol. Eng. 17, 507–520.

Kraus, K., Pfeifer, N., 1998. Determination of terrain models in wooded areas with airborne laser scanner data. ISPRS J. Photogramm. Remote Sensing 53, 193–203.

Lane, S.N., James, T.D., Pritchard, H., Saunders, M., 2003. Photogrammetric and laser altimetric reconstruction of water levels for extreme flood event analysis. Photogramm. Rec. 18, 293–307.

Legleiter, C.J., Overstreet, B.T., 2012. Mapping gravel bed river bathymetry from space. J. Geophys. Res.-Earth Surf. 117, F04024.

Lejot, J., Delacourt, C., Piegay, H., Fournier, T., Tremelo, M., Allemand, P., 2007. Very high spatial resolution imagery for channel bathymetry and topography from an unmanned mapping controlled platform. Earth Surf. Process. Landforms 32, 1705–1725.

Liu, Y., Zhou, J., Song, L., Zou, Q., Guo, J., Wang, Y., 2014. Efficient GIS-based model-driven method for flood risk management and its application in central China. Nat. Hazards Earth Syst. Sci. 14, 331–346.

Longuet-Higgins, H., 1981. A computer algorithm for reconstructing a scene from two projections. Nature 293, 133–135.

Luong, Q.T. 1992. Matrice Fondamentale et Calibration Visuelle sur l'Environnement-Vers une plus grande autonomie des systemes robotiques. PhD Thesis. Université de Paris-Sud, Centre d'Orsay, France, 256 pp.

Luong, Q.T., Faugeras, O.D., 1996. The fundamental matrix: theory, algorithms, and stability analysis. Int. J. Computer Vision 17, 43–75.

MAGRAMA. 2011. Guía metodológica para el desarrollo del Sistema Nacional de Cartografía de Zonas Inundables. Ministerio de Agricultura, Alimentación y Medio Ambiente. Gobierno de España, Madrid, Ministerio de Agricultura, Alimentación y Medio Ambiente. Gobierno de España.

MAGRAMA. 2014 <http://www.magrama.gob.es/es/agua/temas/gestion-de-los-riesgos-de-inundacion/> (Accessed 21.10.14).

Marcus, W.A., Fonstad, M.A., 2008. Optical remote mapping of rivers at sub-meter resolutions and watershed extents. Earth Surf. Process. Landforms 33, 4–24.

Marcus, W.A., Fonstad, M.A., 2010. Remote sensing of rivers: the emergence of a subdiscipline in the river sciences. Earth Surf. Process. Landforms 35, 1867–1872.

Martínez, A., Salas, J.D., 2004. Modelación estocástica de lluvias horarias. Ingeniería del agua 11, 29.

Martínez Marín, E. 2001. Hidráulica Fluvial. Principios y Práctica. HIDRÁULICA. Biblioteca Técnica Universitaria. España, BELLISCO, pp. 213–216.

Merwade, V., Cook, A., Coonrod, J., 2008a. GIS techniques for creating river terrain models for hydrodynamic modeling and flood inundation mapping. Environ. Model. Software 23, 1300–1311.

Merwade, V., Olivera, F., Arabi, M., Edleman, S., 2008b. Uncertainty in flood inundation mapping: current issues and future directions. J. Hydrol. Eng. 13, 608–620.

MFOM. 2014 <http://www.idee.es/web/guest/europeo-inspire> (Accessed 11.11.14).

Mikolajczyk, K., Schmid, C., 2005. A performance evaluation of local descriptors. IEEE Trans. Pattern Anal. Mach. Intell. 27, 1615–1630.

Ministerio de la Presidencia. 2010. Real Decreto 903/2010, de 9 de julio, de evaluación y gestión de riegos de inundaciones. RD 903/2010.

Molina, J.L., Pulido-Velazquez, D., Garcia-Arostegui, J.L., Pulido-Velazquez, M., 2013. Dynamic bayesian networks as a decision support tool for assessing climate change impacts on highly stressed groundwater systems. J. Hydrol. 479, 113–129.

Molina, J.L., Rodriguez-Gonzalvez, P., Carmen Molina, M., Gonzalez-Aguilera, D., Espejo, F., 2014. Geomatic methods at the service of water resources modelling. J. Hydrol. 509, 150–162.

Montgomery, D.C., Runger, G.C., 2006. Probabilidad y estadística aplicadas a la ingeniería. Limusa Wiley, México.

Ng, W.W., Panu, U.S., 2010. Comparisons of traditional and novel stochastic models for the generation of daily precipitation occurrences. J. Hydrol. 380, 222–236.

Nkurunziza, M., Vermeire, L. 2014. A comparison of outlier labeling criteria in univariate measurements (Contributed Paper). In: ICOTS9 9th International Conference on Teaching Statistics. 13–18 July 2014 Flagstaff, Arizona, USA.

Norbiato, D., Borga, M., Sangati, M., Zanon, F., 2007. Regional frequency analysis of extreme precipitation in the eastern Italian Alps and the August 29, 2003 flash flood. J. Hydrol. 345, 149–166.

Ortega-Terol, D., Moreno, M.A., Hernández-López, D., Rodríguez-Gonzálvez, P., 2014. Survey and classification of large woody debris (LWD) in streams using generated low-cost geomatic products. Remote Sensing 6 (12), 11770–11790.

Prinos, P. 2008. Review of flood hazard mapping. Floodsite Report No. T03-07-01, Spain, FLOODsite. Integrated Flood Risk Analysis and Management Methodologies.

Rieke-Zapp, D.H., Nearing, M.A., 2005. Digital close range photogrammetry for measurement of soil erosion. Photogramm. Rec. 20, 69–87.

Sayers, P.B., Hall, J.W., Meadowcroft, I.C., 2002. Towards risk-based flood hazard management in the UK. Proc. Inst. Civil Eng.-Civil Eng. 150, 36–42.

Schmidt, K.A., Hadley, B.C., Wijekoon, N., 2011. Vertical accuracy and use of topographic LIDAR data in coastal marshes. J. Coast. Res. 27, 116–132.

Snavely, N., Simon, I., Goesele, M., Szeliski, R., Seitz, S.M., 2010. Scene reconstruction and visualization from community photo collections. Proc. IEEE 98, 1370–1390.

Tola, E., Lepetit, V., Fua, P., 2010. DAISY: an efficient dense descriptor applied to wide-baseline stereo. IEEE Trans. Pattern Anal. Mach. Intell. 32, 815–830.

Tsakiris, G., 2014. Flood risk assessment: concepts, modelling, applications. Nat. Hazards Earth Syst. Sci. 14, 1361–1369.

Tsubaki, R., Fujita, I., 2010. Unstructured grid generation using LiDAR data for urban flood inundation modelling. Hydrol. Process. 24, 1404–1420.

Turner, A.B., Colby, J.D., Csontos, R.M., Batten, M., 2013. Flood modeling using a synthesis of multi-platform LiDAR data. Water 5, 1533–1560.

US Army Corps of Engineers. 2010. HEC-RAS. River analysis system hydraulic. Hydraulic reference manual.

Vallet, J., Panissod, F., Strecha, C., Tracol, M. 2011. Photogrammetric performance of an ultra light weight swinglet "UAV". In: Conference on Unmanned Aerial Vehicle in Geomatics, Zurich, Switzerland. International Archives of the Photogrammetry, Remote Sensing and Spatial Information Sciences, vol. XXXVIII-1/C22 UAV-g 2011.

Warren, I.R., Bach, H.K., 1992. MIKE 21: a modelling system for estuaries, coastal waters and seas. Environ. Software 7, 229–240.
Watts, A.C., Perry, J.H., Smith, S.E., Burgess, M.A., Wilkinson, B.E., Szantoi, Z., et al., 2010. Small unmanned aircraft systems for low-altitude aerial surveys. J. Wildl. Manage. 74, 1614–1619.
Wechsler, S.P., 2007. Uncertainties associated with digital elevation models for hydrologic applications: a review. Hydrol. Earth Syst. Sci. 11, 1481–1500.
Wiles, J., Levine, N., 2002. A combined GIS and HEC model for the analysis of the effect of urbanization on flooding: the swan creek watershed, Ohio. Environ. Eng. Geosci. 8, 47–61.
Yang, T., Shao, Q., Hao, Z., Chen, X., Zhang, Z., Xu, C., et al., 2010. Regional frequency analysis and spatio-temporal pattern characterization of rainfall extremes in the Pearl River Basin, China. J. Hydrol. 380, 386–405.
Zazo, S., Rodríguez-Gonzálvez, P. 2014. Estudio de la aplicación de la tecnología de aeronaves ultraligeras motorizadas (tipo ULMs), de coste reducido y baja altura de vuelo, en vuelos fotogramétricos de detalle, para Estudios y Proyectos Hidráulicos y/o de Ingeniería Fluvial. Unpublished Tesis Fin de Máster. Universidades de Salamanca y Valladolid.
Zechner, S., Grossmann G., Pohl R., Natale L., Escuder Bueno, I., Bateman, A. 2011.Guidance. SUFRI Methodology for investigation of risk awareness of the population concerned. 2nd ERA-Net CRUE Funding Initiative European Flood Risk.